

Research Paper

Liquefaction-Induced Settlement and Lateral Spreading Effects on Buried Pipelines by Using Shaking Table Tests

Mohammad Ahmadi* and Abbas Ghalandarzadeh²

1. Assistant Professor, Department of Civil Engineering, Faculty of Civil Engineering and Architecture, Malayer University, Malayer, Iran,

*Corresponding Author; email: m.ahmadi@malayeru.ac.ir

2. Professor, School of Civil Engineering, University of Tehran, Tehran, Iran

Received: 15/04/2023

Revised: Not Required

Accepted: 18/04/2023

ABSTRACT

Keywords:

Buried pipeline;
Liquefaction; Settlement;
Lateral spreading;
1-g shaking table

Due to the importance of buried pipelines as one of the types of lifelines, it is necessary to consider all possible seismic hazards in their operation. Settlement and lateral spreading caused by liquefaction are among these risks. In this research, their effects have been investigated using two series of 1-g shaking table tests. Results show that the maximum displacement applied to the pipe occurs during the shake is greater than the residual displacement after the shake. Also, by investigating the shear stress-shear strain curves (hysteresis loop), the reduction of shear stiffness due to the shake was observed. After liquefaction occurs, the soil loses its shear strength, and the slope starts to move downstream. It is observed that the contribution of cyclic strains due to the ground vibration is far less than the contribution of strain due to monotonic displacement. According to the findings of this research, the deformation of the pipe is less than the settlement of the ground due to the liquefaction.

1. Introduction

Today, pipelines, both as distribution networks and as transmission lines, play a special role in modern urban life, which is why they are classified as lifelines. On the one hand, the transfer of water, gas, liquid fuel, etc. for the residents of the cities and the exit of sewage from the cities clearly shows the essential role of pipelines. The creation of any damage that leads to disruption of the performance of distribution lines and networks will bring irreparable socio-economic damages. Meanwhile, buried gas pipelines are more important due to possible risks in case of damage.

Among the factors that can damage pipelines is the occurrence of an earthquake. The investigation of past earthquakes shows that buried pipes have suffered severe damage due to the consequences

of earthquakes such as liquefaction (Hamada et al., 1996).

In general, an earthquake can damage buried pipes in two ways. One category of these damages is related to the phenomenon of earthquake wave propagation, and the other category is related to permanent ground displacement (PGD) (Sun et al., 2009). As a result of an earthquake, permanent ground displacement can happen in different ways. Surface faulting, landslides, lateral spreading and vertical settlement caused by liquefaction are among the events that can cause permanent ground displacement. The phenomenon of lateral spreading on slopes occurs when the loose and fully saturated sandy soil becomes liquefied due to ground shaking and the slope begins to move to its downstream

side. Due to the occurrence of liquefaction, the soil loses its shear resistance and begins to flow and move down the slope due to its own weight. This phenomenon can happen even on very low slopes (0.5 to 1%). Apart from the phenomenon of lateral spreading, settlement caused by liquefaction, even when the ground is flat, can cause permanent ground displacement, as a result of which it can exert bending forces on the pipe that is buried.

Due to the importance of the problem, many studies have been conducted on investigating the behavior of liquefaction on buried pipelines using physical modeling by using 1-g shaking table tests (Ko et al., 2023; Otsubo et al., 2016; Qiao et al., 2008; Ecemis et al., 2021; Castiglia et al., 2021). Since lifelines are long structures that pass through different areas with different topographies and are generally buried at a small depth, it is possible for them to pass through slopes with the possibility of liquefaction. Various researchers have investigated the effect of lateral spreading caused by liquefaction on buried pipelines (O'Rourke & Lane, 1989; Lim et al., 2001; Papadimitriou et al., 2019).

In this research, the effect of permanent deformations caused by liquefaction on buried gas pipelines is investigated in two cases. The first case is the occurrence of lateral spreading caused by liquefaction on low slopes and the investigation of its effect on buried pipes, and the second case is the investigation of the effect of settlement caused by liquefaction on flat lands. This investigation has been done by designing and implementing

several physical model tests using a 1-g shaking table.

2. Physical Model Tests Using 1-g Shaking Table

In this research, to investigate the phenomenon of liquefaction, the physical modeling method was used by a one degree of freedom 1-g shaking table test. This device was developed in the Soil Mechanics Laboratory of Tehran University. This device has different parts, including a deck, hydraulic actuator, power unit, and control and measurement system. The system deck, on which the model is placed, is moved by a hydraulic actuator. This stimulation is caused by a hydraulic power unit. Figure (1) shows the shaking table used along with one of the models prepared on it.

2.1. Soil Box

The models are made inside a transparent plexiglass box so that the deformation of the model due to the earthquake can be easily observed. The dimensions of the used box are 180 cm in length, 45 cm in width, and 70 cm in height, and the thickness of the plexiglass is 2 cm. At both ends of the bottom of the box, there are two taps that can add carbon dioxide (CO₂) and water to the sample. The use of carbon dioxide is to ensure the full saturation of the soil in the models.

2.2. Transducers

Five series of transducers (accelerometers, LVDTs, string potentiometers, pore water pressure gauges and strain gauges) are planned to record

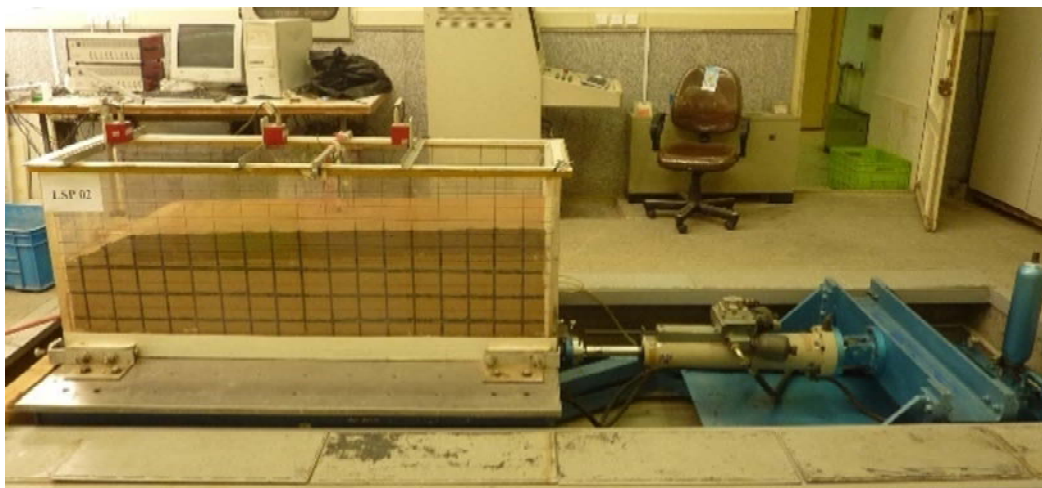


Figure 1. 1-g shaking table test used in current study.

test data in these models. Five accelerometers were used in these models. One of the accelerometers was installed outside the box and near its bottom to measure the base acceleration applied to the sample. Four other sensors were installed in the soil at depths of 10, 20, 30 and 40 cm from the ground surface. Using data obtained from these accelerometers, it is possible to study the response of the ground as well as the occurrence of liquefaction phenomena at different soil levels. String potentiometers have been used to calculate the displacement of the buried pipe. The cables of these sensors were connected to two points on the pipe, and the deformation of the pipe was recorded. In addition, one of the sting potentiometers, by using a buried element inside the soil, recorded the movement and lateral deformation of the soil in the experiments to investigate the effect of lateral spreading.

Also, LVDTs have been used to calculate ground surface displacements in the vertical direction. The ground surface displacement was measured by three displacement gauges at different points. In this research, three pore water pressure sensors were used to record changes in pore water pressure during and after the earthquake at depths of 20, 30 and 40 cm from the ground. Also, to measure the compressive and tensile strains and calculate the bending moments in the pipe, a series of strain gauges was installed in three sections of the pipeline. Two 10-channel dynamic data loggers were used to collect and record the 20 sensors used in this experiment. The data loggers are DRA-101C and manufactured by Tokyo Sokki Kenkujo. Figures (2) and (3) show the sensors used in this research. Also, the location of these sensors is specified in Figure (4).

2.3. Modeled Soil

To prepare a soil in which liquefaction can be observed, clean sands with d_{50} less than 0.5 mm have been used in many studies. For example, Toyora sand in Japan and Nevada sand in America are used in almost the same studies. Firoozkooh sand No. 161, which is very similar to the aforementioned sands in terms of grain size and other characteristics, was used in this research. Table (1) shows its physical characteristics.

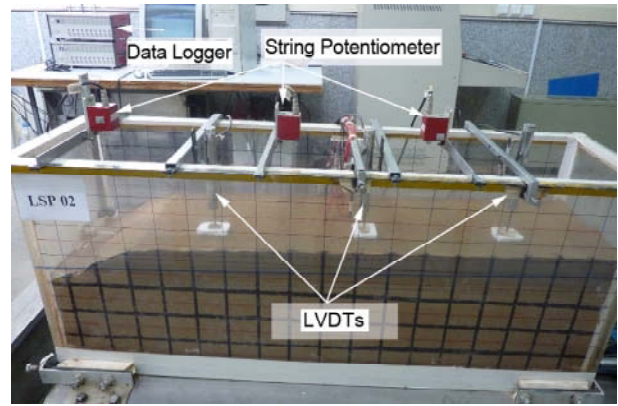
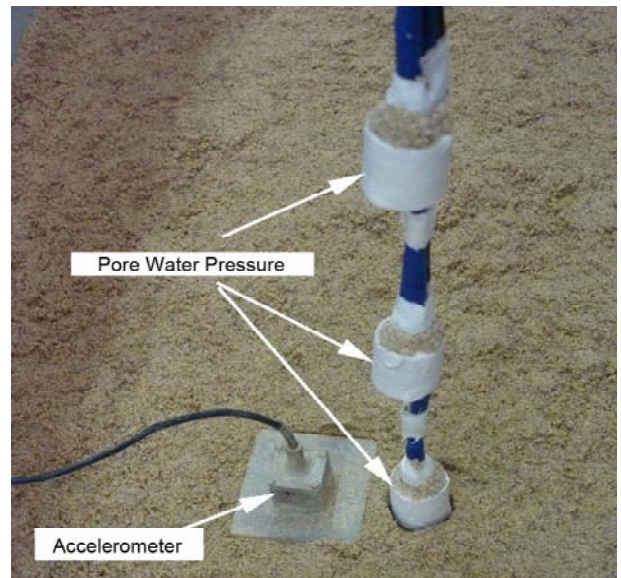
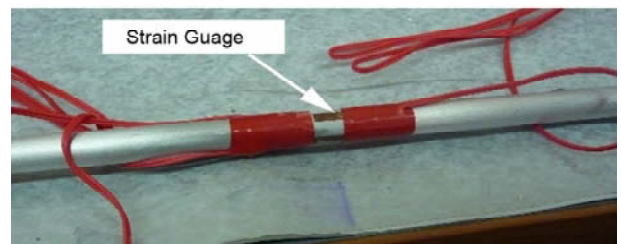


Figure 2. Different types of LVDT transducers used in current study.



(a)



(b)

Figure 3. (a) pore water pressure sensors and accelerometers (b) Strain gauge connected to the model pipe.

Table 1. Physical characteristics of Firoozkooh 161 sand used in current research.

Parameter	Value	Unit
G_s	2.658	-
e_{max}	0.943	-
e_{min}	0.603	-
d_{50}	0.3	mm
Fine Percent	Zero	%
Internal Friction Angle (ϕ)	37	Degree
Cohesion (c)	zero	kPa

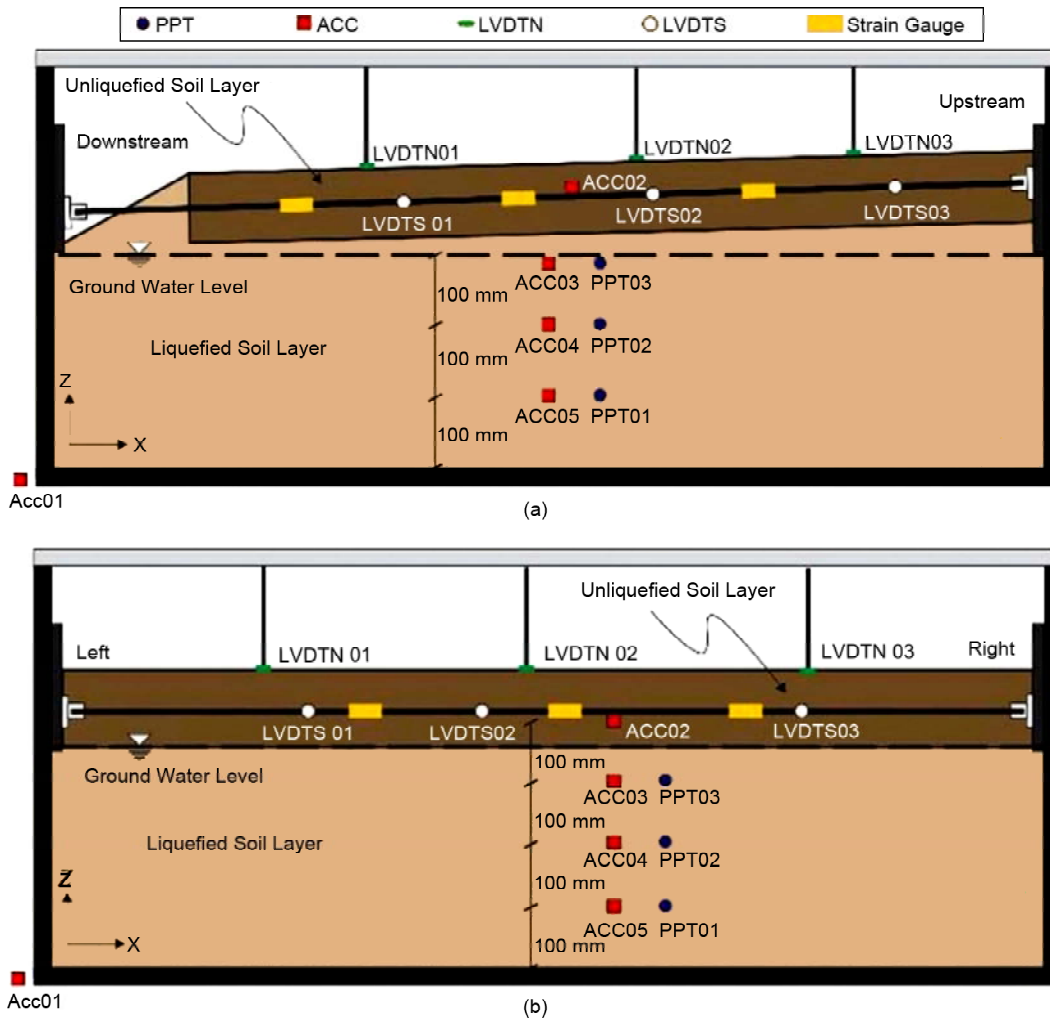


Figure 4. Model geometry and its instrumentation map for a) lateral spreading models; b) for models to investigate the effect of settlement (Nourzadeh et al., 2019).

Since in these tests the pipe is buried inside a non-liquefiable layer, this layer was made of a mixture of 161 Firoozkooh sand with 15% kaolinite clay.

2.4. Modeled Pipe

Using the scaling law (Section 2-5), the aluminum pipe with the specifications presented in Table (2) was chosen as the most suitable pipe to model a steel pipe with a diameter of 14 inches and a thickness of 17.8 mm in prototype scale.

Table 2. Physical characteristics of the pipe used in the model.

Parameter	Value	Unit
Pipe Material	Aluminum	-
Pipe Diameter	10	mm
Pipe Thickness	0.5	mm
Pipe Length	1.70	m
Modulus of Elasticity	74	GPa

2.5. Scaling Laws

Soil behavior is a function of confining stress, and by reducing the dimensions of the model by n (the scaling factor), the level of stresses in the small-scale physical model is reduced compared to the prototype. Therefore, in order for the data obtained from the laboratory model test to be generalizable to the large-scale model, a series of rules, known as scaling laws, must be used. In the current research, according to the seismic nature of the problem and the presence of liquefaction, appropriate scale laws have been used (Iai, 1989). The similarity ratio in this research is $n = 35$. Table (3) shows the similarity laws used in the current study.

2.6. Geometry of Model

In the current research, the buried pipe is located in a layer of non-liquefiable soil, and

Table 3. Similarity laws between small-scale model and prototype in current study.

Parameter	Scaling Factor	Value
Length	n	35
Strain in Soil	$n^{0.5}$	5.9
Pore Water Pressure	n	35
Displacement	$n^{1.5}$	207
Acceleration	1	1
Flexural Rigidity (Per Unit Length)	$n^{4.5}$	8877817
Axial Rigidity (Per Unit Length)	$n^{1.5}$	207

beneath this layer, liquefiable soil is present (American Lifeline Alliance (ALA), 2001). In the tests to investigate the effect of lateral spreading, the slope direction is parallel to the length of the buried pipe. However, in the tests to investigate the settlement effect, the ground surface is flat and has no slope. Figure (4a) shows the geometry of the model in the experiments. The only difference in the tests is the slope of the ground, and the location of the sensors remains unchanged. The pipe is buried at a depth of 5 cm, according to the similarity ratio of 35 times, but in reality it will be located at a depth of about 1.75 m, which corresponds to the prototype.

Figure (4b) depicts the model's geometry and instrumentation for looking into the effects of liquefaction-related settlement. In these figures, PPT shows the location of pore water pressure sensors, ACC of acceleration sensors, LVDTN of vertical displacement sensors, and LVDTs of string LVDT. The position of the strain gauges is also marked on the pipe in this figure.

2.7. Testing Program

As mentioned before, in the current study, two series of physical models were planned to investigate the effect of lateral spreading and settlement caused by liquefaction. In experiments to investigate the effect of lateral spreading, the

slope of the ground is variable. The test schedule is presented in Table (4).

2.8. Sample Preparation

In this research, the physical model is prepared based on the wet compaction method. In this method, to reach the desired density, about 5% moisture is added to the soil and mixed well with the soil to prepare a uniform material. Then, for a specific volume of soil in the box, the required soil mass is calculated. Then, using special hammers, a number of uniform blows are applied to the model so that this amount of soil is compacted into the specified volume. With this method, a uniform sample with the required density percentage can be created. A network of lines created with colored sands was used to observe soil deformations. After preparing the soil sample, drilling is done to the required depth to install the gas pipe, and after installation, the pipe is covered with the soil. Then the soil is saturated by adding water from the bottom of the model. Air trapped between soil pores cannot easily dissolve in water. Thus, passing CO₂ gas through the model for a few hours and replacing it with air causes that after water passes through the sample, this gas is dissolved in water and all soil pores are saturated with water. The final step is to apply the desired shake to the model and record the data using the installed transducers. Figure (5) shows the process of model preparation.

3. Results

In this section, the most important results obtained from physical models are discussed.

3.1. General Observations in the Models

What has been observed in all the lateral

Table 4. Testing program.

Test	Ground Slope (%)	Exerted Acceleration (g)	Time of Shaking (s)	Frequency of Shaking (Hz)	Relative Density of Soil (%)
LSP01	4	0.2	5	3	21
LSP02	2.5	0.2	5	3	16
LSP03	1.5	0.2	5	3	13
LSP04	zero	0.2	5	3	13
LSP05	zero	0.25	5	3	57
LSP06	zero	0.5	7	5	57

spreading tests is the movement of the slope towards the bottom of the slope after applying the earthquake and the occurrence of complete liquefaction in the model. This change is clearly shown in the pictures taken from outside the soil box and by the colored

sands. The verticality of colored sand layers in the upper layer where the pipe is buried shows that this layer is not liquefied. The movement of the non-liquefiable layer towards the bottom of the slope due to the liquefaction of the underlying soil causes axial and bending forces in the buried pipes. Figure (6) shows a view of the prepared model before the shake and also the deformations created in the soil after the shake for test LSP01.

In the liquefaction-induced settlement experiments, as expected, the ground surface experienced significant settlement when complete liquefaction occurred. Also, the phenomenon of sand boiling has been clearly observed in the models. Figure (7) shows the occurrence of liquefaction and land subsidence in one of the models with a flat surface. The phenomenon of sand boiling and the movement of sand particles towards the upper layers can be seen in the transparent wall of the model, some of

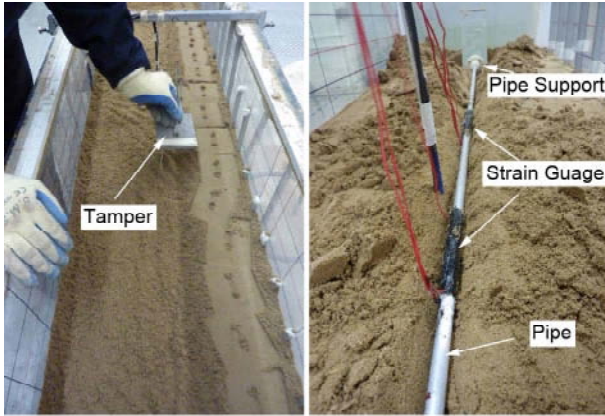
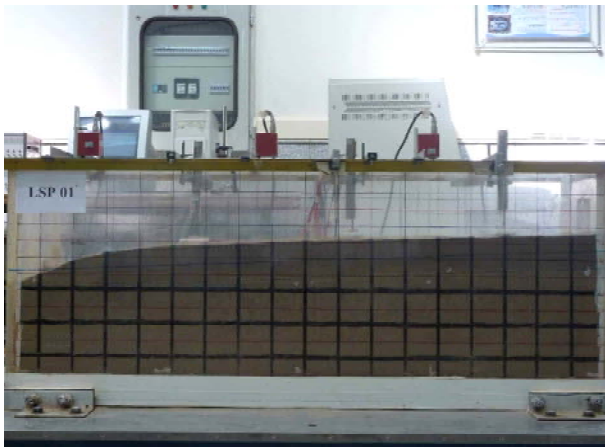
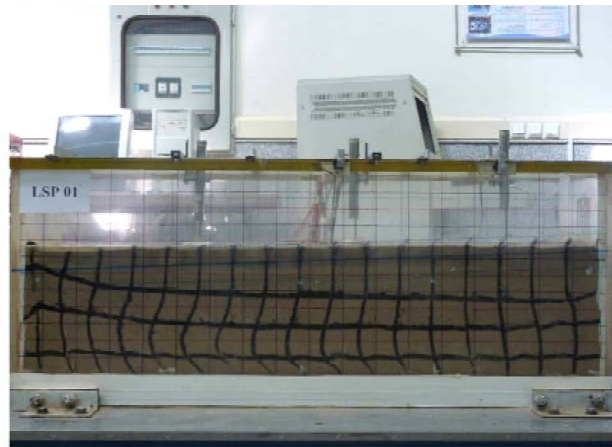


Figure 5. Model preparation process.

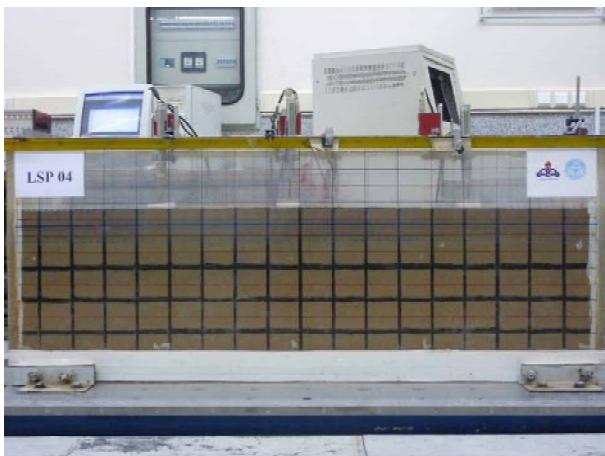


(a) Before Shake

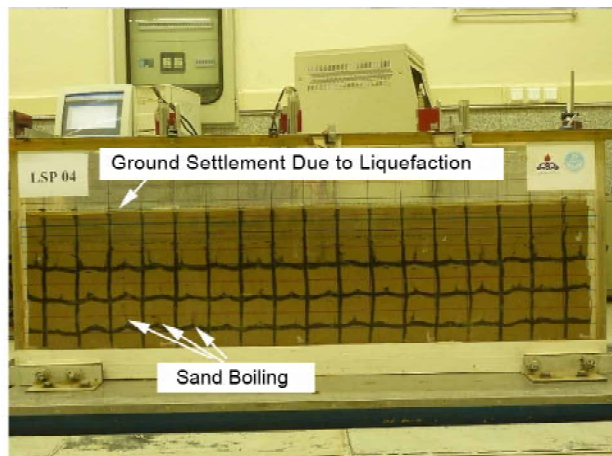


(b) After Shake

Figure 6. Physical model to investigate the effect of lateral spreading (LSP01).



(a) Before Shake



(b) After Shake

Figure 7. Physical model to investigate the effect of settlement due to liquefaction (LSP04).

which are shown in Figure (6). Observing this phenomenon in the whole model indicates the homogeneity of the soil and the occurrence of complete liquefaction in all its parts.

3.2. Shear Stress-Shear Strain Curves (Hysteresis Loop)

In order to investigate the dynamic performance of the soil around the pipe during vibration, shear stress-strain curves, known as hysteresis loops, were calculated for different soil depths. Figure (8) shows the hysteresis loops for samples with

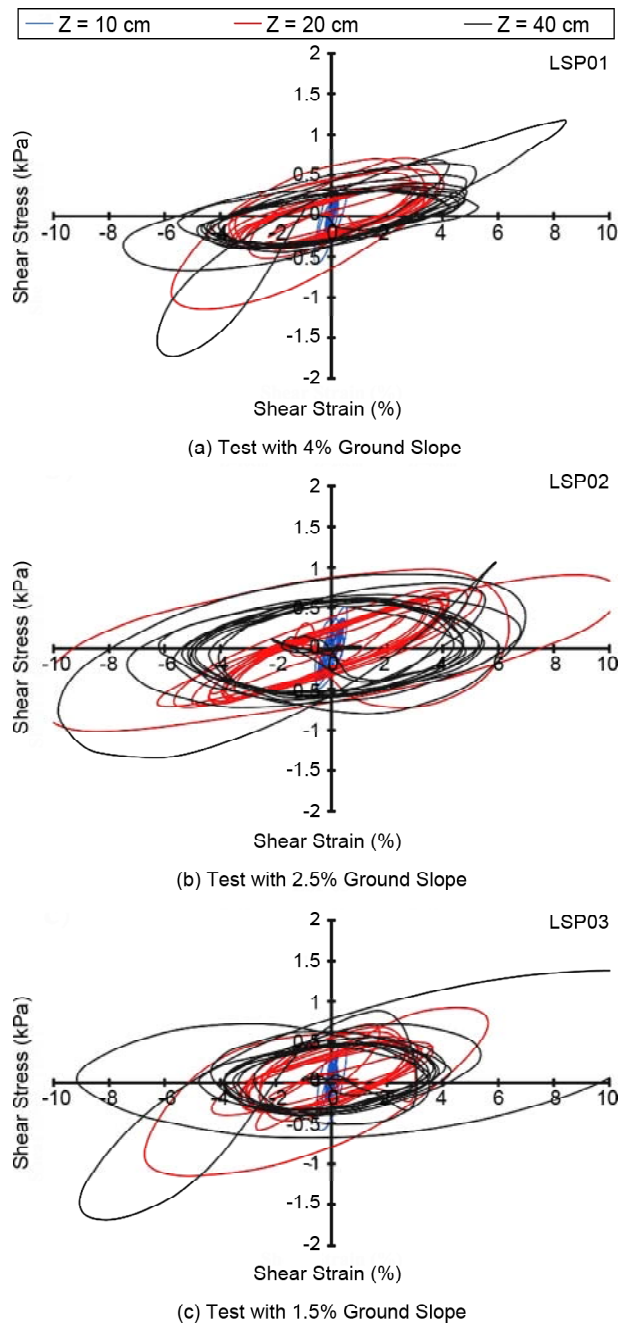


Figure 8. Shear stress - shear curve at depths of 10, 20 and 40 cm from the surface of the model.

slopes at three depths of 10, 20 and 40 cm (in blue, red and black colors, respectively) from the ground surface. In all these tests, it can be seen that with increasing depth, the maximum shear strain produced during shaking increases. The reason is the higher deformation of the lower layers than the surface layers. This issue is clearly seen in the images taken from the models during the earthquake, which can be seen by the colored horizontal and vertical lines in the model. The reason for the significant difference between the shear stress-shear strain curve at a depth of 10 cm and the rest of the depths is the location of the acceleration sensor in the non-liquefiable layer. Due to the lack of liquefaction of the soil in this layer, the shear strains created during an earthquake are much less than in areas that have undergone liquefaction.

Another important point is the reduction of soil shear modulus (G) with the onset of liquefaction. The secant shear modulus, which is the slope of the maximum point in the hysteresis curve in each of the rings, decreases with increasing depth. On the other hand, with the increase in loading cycles at any point, the reduction of the secant shear modulus is clearly observed. This trend can be seen in all the curves in Figure (8).

Another point is that by reducing the slope of the land, the maximum shear strain decreases during an earthquake. Shear strain has a direct relationship with the deformation of the model, and in models with a higher ground slope, the displacement of liquefied layers is greater than in a model with a lower ground slope.

Figure (9) shows the shear stress - shear strain curve at depths of 10, 30 and 40 cm from the surface of the model to test the effect of liquefaction settlement on pipelines in flat ground (LSP06). As in the tests on sloping ground, the shear strain in liquefied soil is much higher than in non-liquefied soil. Also, a significant difference is observed in the shear modulus of the soil after the start of liquefaction in these two layers. The decrease of the shear modulus at each depth with the increase of loading cycles is also well visible in the graphs. Another important point is that the shear modulus of the soil at a depth of 30 cm after complete liquefaction has become lower than at a depth of

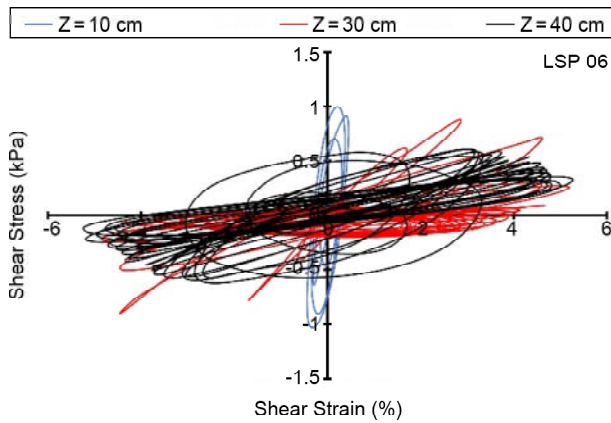


Figure 9. Shear stress - shear curve at the depths of 10, 30 and 40 cm from the surface of the LSP06 test model.

40 cm. The reason for that is the lower confining pressure of the soil at a depth of 30 cm compared to a depth of 40 cm. The conclusion that can be drawn from these diagrams is the importance of considering the reduction of shear stiffness in liquefied soil in numerical models, which can strongly affect its results.

3.3. Diagrams of Acceleration-Lateral Displacement of Soil in the Models for Investigating the Effect of Lateral Spreading

Lateral spreading caused by liquefaction on slopes depends on two factors. The first factor is the application of acceleration due to the earthquake to the soil layers, and the second factor is the reduction of soil shear stiffness (also known as soil softening) and the loss of its shear resistance due to liquefaction. Displacement is a function of both factors. The applied acceleration causes inertial forces and, as a result, permanent soil deformation. On the other hand, the softening of the soil causes the gravitational forces to cause permanent deformation in the soil. In order to understand the effect of these two factors on soil deformations, which affect the behavior of the buried pipe, diagrams of acceleration against lateral displacement of the soil have been drawn. Figures (10), (11) and (12) show the relationship between the base acceleration and the acceleration induced in the soil against the horizontal displacement. The location of the lateral displacement sensor and the accelerometer closest to it are shown in Figure (4). This sensor is located at a height equal to the height of the ACC02 accelerometer and inside the non-liquefiable soil.

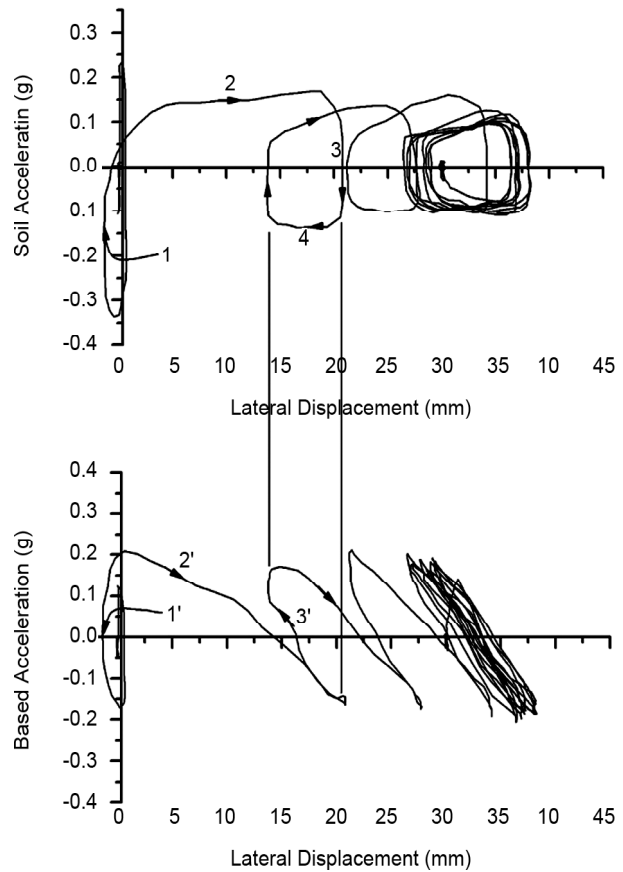


Figure 10. Acceleration-Lateral displacement curve for LSP01 test with 4.5% ground slope.

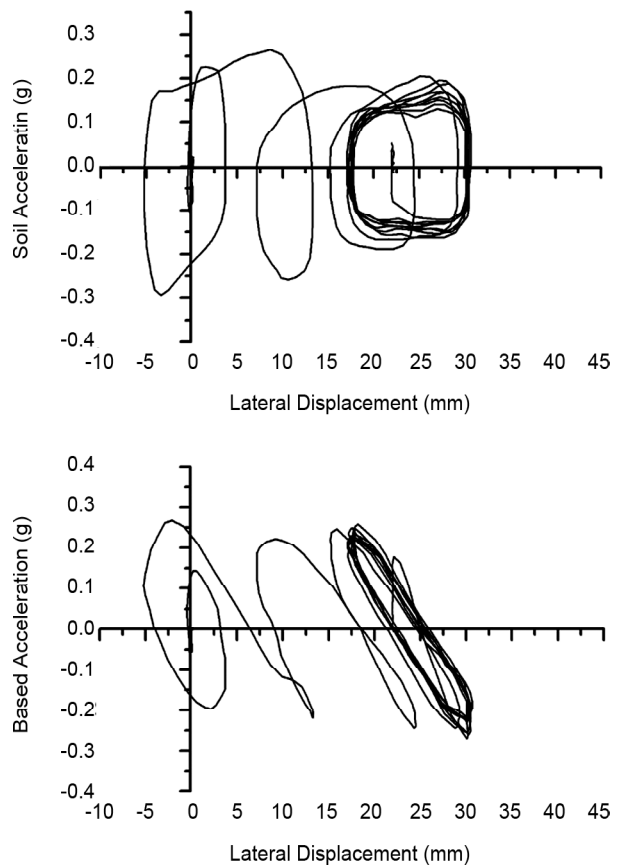


Figure 11. Acceleration-Lateral displacement curve for LSP02 test with 2.5% ground slope.

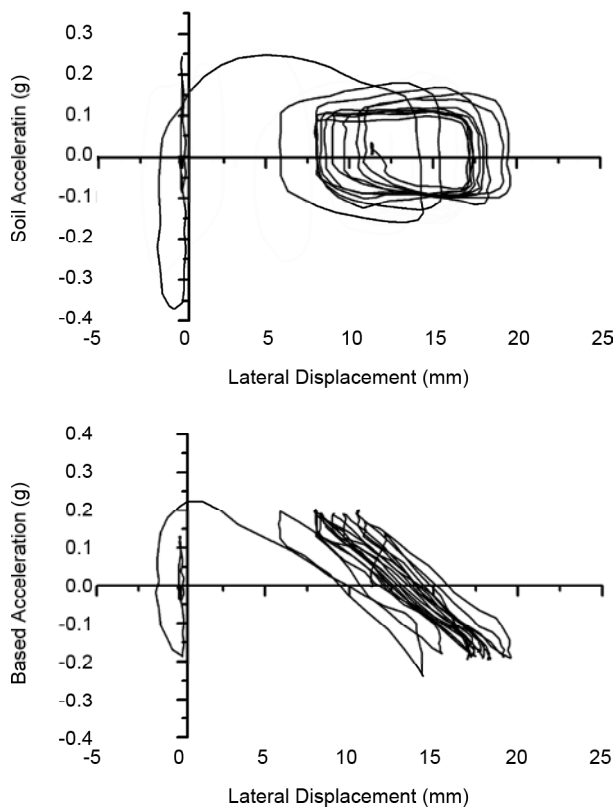


Figure 12. Acceleration-Lateral displacement curve for LSP03 test with 1.5% ground slope.

As can be seen in these figures, for all experiments, a rapid increase in displacement occurs in the first few cycles. In other words, the lateral spreading occurred mainly in the first cycles during the application of shaking. This phenomenon is common in soils that are very prone to liquefaction, and the pore water pressure increases to a maximum value during the first few cycles. In these soils, deformations can continue even after the shaking stops. However, in the experiments conducted due to the limitation of the length of the test box, the lateral movement of the slope almost stopped after the shaking.

It is noteworthy to compare the effect of the base acceleration and the acceleration recorded in the soil on the lateral movement of the soil. According to the numbered steps on the curves for the LSP01 test, this difference is explained. In stage 1, since the acceleration recorded in the soil changes from negative to positive, despite the increase in acceleration, no significant displacement occurs, but in the part of the curve where the acceleration reached its maximum value, a very large displacement occurs. This indicates that in this state, the soil is in its softest state, and because

the pore water pressure is at its maximum value, the soil undergoes large deformations due to the extremely high softening and the simultaneous effect of the gravitational force caused by the slope of the earth (step 2). With the continuation of the shear deformation and the change in the direction of acceleration, the forward movement of the soil suddenly stops (stage 3), but due to the effect of negative acceleration in stage 4, a small part of the deformation of the ground occurs in the direction of reduction. In fact, this curve and similar curves in other tests show the appropriate adaptation of acceleration, displacement, and soil softening.

The relationship between the lateral movement of the soil and the base acceleration has a different trend. As seen in the curve related to the LSP01 test, in the first cycle, in step 1, the increase in base acceleration caused a small displacement in the soil, but in the deceleration phase in step 2, despite the decrease in base acceleration, the displacement increased. In fact, despite the reduction of the inertial force due to the acceleration, displacement has occurred, which is significant. This movement is actually caused by the softening of the soil due to liquefaction or the increase in pore water pressure. An interesting point can be seen in step 3: despite the increase in acceleration, the direction of displacement has been reversed. This shows that due to liquefaction, there is a strong phase difference between the acceleration applied to the soil and the base acceleration. This phase difference is caused by the extreme softening of the soil and the occurrence of very high damping due to liquefaction. However, the process of changes in basic acceleration and lateral movement of soil is also logical and can be explained. The important point of observing these curves is the occurrence of the highest displacement in the first cycles, which occurs in soils with high liquefaction potential. At this stage, there is a possibility that the forces on the pipe will be significant. However, because this movement occurs in a situation where the soil is very soft, it can reduce some of the forces on the pipe. However, if the pipe is in a layer that does not undergo liquefaction but, due to the liquefaction of the lower layers, its movement is significant, the forces acting on the pipe can be significant.

The result of examining the curves of the effect

of acceleration on lateral displacement can be summarized in the following cases: 1- The displacement of the slope is affected by two factors: inertia forces on one side and gravity forces due to soil softening on the other side. 2- In soils with high liquefaction potential, the most displacements occur in the first few cycles. 3- A significant part of the displacement occurs during the shaking, but although the continuation of deformations in the laboratory observations is insignificant due to the limited dimensions of the model, lateral displacements can also occur to some extent after the termination of the ground shaking. 4- The softening caused by liquefaction creates a significant phase difference in the soil movement in the liquefied area compared to the applied movement (base acceleration).

The forces caused by this displacement have an impact on the buried pipe due to the effects of soil displacement from applied acceleration and displacement caused by static gravity forces. Due to the dynamic and monotonic nature of soil deformation (caused by gravity loads and soil softening), both types of ground displacement can have an impact on the forces and deformations applied to buried pipes.

3.4. Diagrams of Soil Lateral Displacement-Axial Strain in Pipe

To evaluate the interaction of the pipe with the soil, lateral soil displacement and axial strain curves are drawn. Figures (13), (14) and (15) show these curves drawn for tests LSP01 to LSP03. These curves are drawn only for the center of the tube near which the horizontal displacement measurement sensor is located. The horizontal axis in these curves is the lateral displacement of the soil, and the vertical axis is the strain on the pipes in percentage. The lateral movement of the slope due to liquefaction causes axial forces in the pipe, which can be accessed and measured in the form of strains recorded by strain gauges in the experiments.

According to the diagrams, two types of axial strain occur during the lateral displacement of the soil. One is the axial strain that occurs during a shake. The nature of these strains is dynamic, and in the first cycles, when the displacement is very high, this amount also increases greatly. But in the

next cycle, it starts to fluctuate within a certain and limited range. The second type of axial strains are the strains applied to the pipe after the end of the shaking. It can be seen that a creep movement in the direction of increasing axial strain occurs slowly after the end of the shaking. The reason for this phenomenon is ground subsidence, which

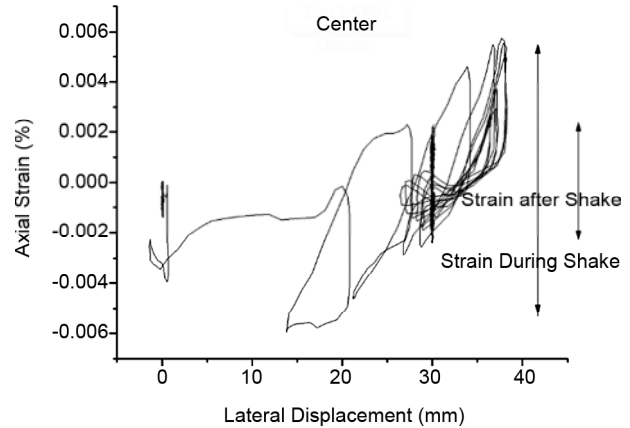


Figure 13. Axial strain in the pipe according to the lateral displacement of the soil for the LSP01 test with a slope of 4.5%.

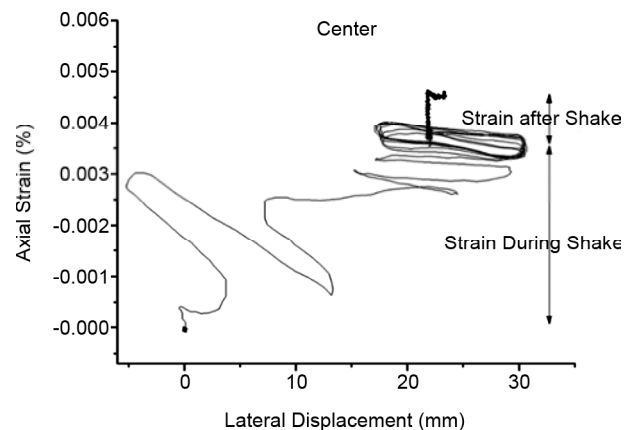


Figure 14. Axial strain in the pipe according to the lateral displacement of the soil for the LSP02 test with a slope of 2.5%

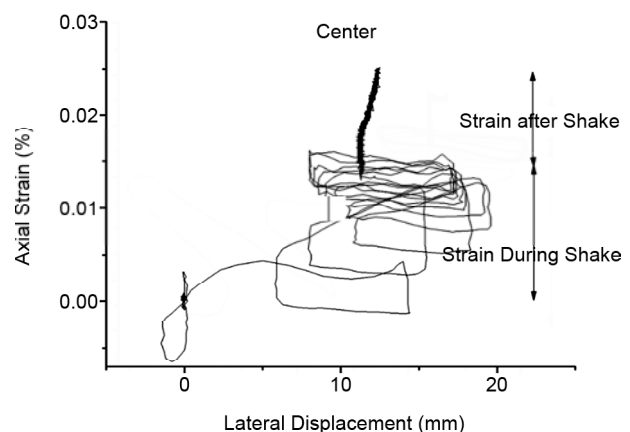


Figure 15. Axial strain in the pipe according to the lateral displacement of the soil for the LSP06 test with a slope of 1.5%.

occurs gradually after liquefaction. This subsidence causes more axial force in the pipes.

3.5. Diagrams of Soil lateral Displacement-Axial Strain in Pipe

As previously mentioned, settlement due to liquefaction in flat lands is a significant factor in causing deformation and force on buried pipes. This issue is less important in the phenomenon of lateral spreading compared to the effect of lateral deformations. In order to investigate the effect of settlement caused by liquefaction and buried pipes, the curves of the vertical displacement of the ground for the vertical displacement of the buried pipe in tests LSP04 to LSP06 are drawn in Figures (16) to (18).

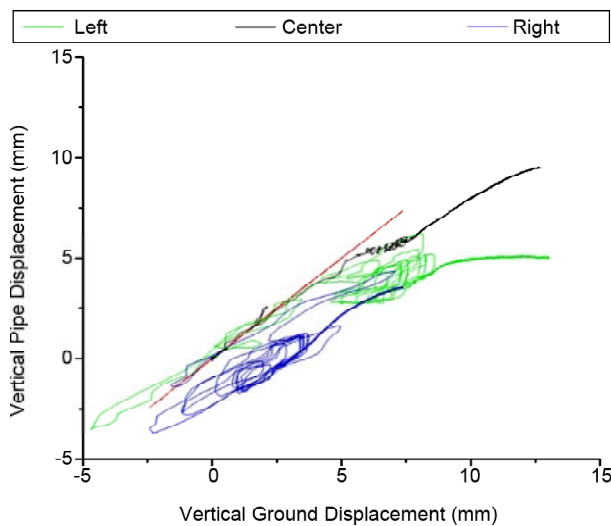


Figure 16. Ground settlement vs vertical displacement of the pipe in LSP04 test.

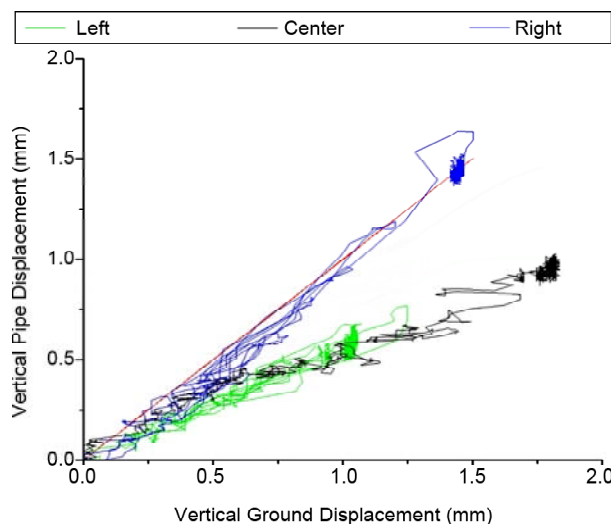


Figure 17. Ground settlement vs vertical displacement of the pipe in LSP05 test.

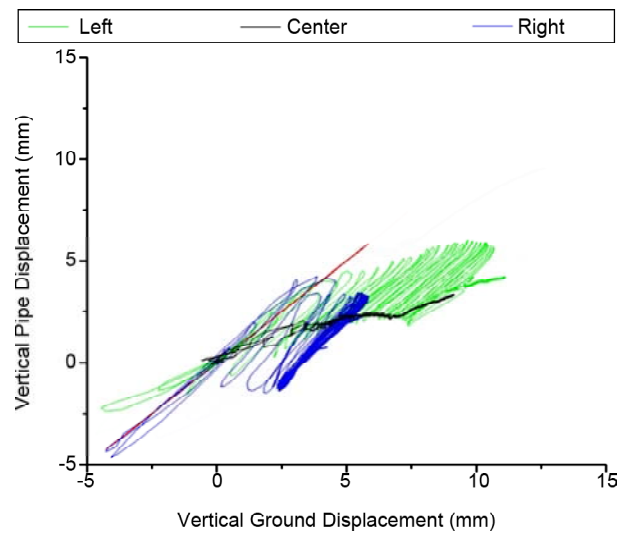


Figure 18. Ground settlement vs vertical displacement of the pipe in LSP06 test.

A red line with an angle of 45 degrees is drawn in the graphs, which indicates that the displacement of the pipe and the vertical displacement of the slope are the same. The important thing that can be concluded from the examination of these diagrams is that in most of these experiments, the change in the vertical position of the ground is greater than the change in the vertical position of the pipe. In fact, most of the curves drawn in this test are located in the lower part of the 45-degree line, which indicates a greater vertical displacement of the ground than the vertical displacement of the pipe at that point. In the numerical analysis of the ground displacement on the pipeline using the spring model, the amount of ground displacement is applied to the springs. Meanwhile, according to the findings of this research, the deformation of the pipe is less than the settlement of the ground due to the liquefaction. As a result, the displacement applied to the pipe in numerical methods is greater than the actual displacement of the pipe. In this case, if there is no damage to the pipes according to the numerical analysis, it can be said with more certainty that no damage will occur in real conditions.

4. Conclusion

In order to investigate the performance of pipes buried in saturated soil that are exposed to liquefaction caused by earthquakes, a series of physical model tests have been conducted to investigate the effect of lateral spreading and

ground settlement caused by liquefaction. Based on the observations made and the recorded data that have been analyzed, the most important results obtained from this study are as follows:

- In the conducted experiments, a significant effect of large deformations of the ground on the pipe has been observed.
- The reduction of soil shear stiffness in hysteresis loops was clearly observed with the continuation of vibration. After the occurrence of liquefaction, the shear stiffness is very low, and the slope starts to move downstream.
- The results show that the important part of the lateral deformations occurs during the application of vibration (earthquake occurrence) and the lesser part after the termination of the vibration until reaching the final residual value.
- According to the results of the tests, the maximum displacement applied to the pipe occurs during the earthquake, and the amount of this displacement is greater than the residual displacement after the earthquake. It seems that the probability of damage to the pipe will be higher in the first moments of the earthquake.
- In the experiments to investigate the effect of lateral spreading, two types of deformation occur. The first type is caused by inertial forces due to applied acceleration. The second type is caused by gravity forces as a result of softening caused by liquefaction, which occurs due to the slope of the ground.
- Among the strains and forces applied to the pipe due to significant softening in the soil, the contribution of cyclic strains due to ground vibration is far less than the contribution of strain due to monotonic displacement (flow rupture). In fact, the dynamic interaction of pipe and soil has a smaller role than the flow displacement interaction of soil and pipe.
- According to the findings of this research, the deformation of the pipe is less than the settlement of the ground due to the liquefaction.

Acknowledgment

The authors would like to express their gratitude to the Research and Technology Office of Tehran Gas Company for the scientific and financial support of this research project.

References

- American Lifeline Alliance (ALA) (2001). Guidelines for the design of Buried steel pipe. *American Society of Civil Engineering (ASCE)*.
- Castiglia, M., de Magistris, F.S., Onori, F., & Koseki, J. (2021). Response of buried pipelines to repeated shaking in liquefiable soils through model tests. *Soil Dynamics and Earthquake Engineering, 143*, 106629.
- Ecemis, N., Valizadeh, H., & Karaman, M. (2021). Sand-granulated rubber mixture to prevent liquefaction-induced uplift of buried pipes: a shaking table study. *Bulletin of Earthquake Engineering, 19*, 2817-2838.
- Hamada, M., Isoyama, R., & Wakamatsu, K. (1996). Liquefaction-induced ground displacement and its related damage to lifeline facilities. *Soils and Foundations, 36*(Special), 81-97.
- Iai, S. (1989). Similitude for shaking table tests on soil-structure-fluid model in 1g gravitational field. *Soils and Foundations, 29*(1), 105-118.
- Ko, Y. Y., Tsai, T.Y., & Jheng, K.Y. (2023). Full-scale shaking table tests on soil liquefaction-induced uplift of buried pipelines for buildings. *Earthquake Engineering & Structural Dynamics, 52*(5), 1486-1510.
- Lim, Y.M., Kim, M.K., Kim, T.W., & Jang, J.W. (2001). The behavior analysis of buried pipeline: Considering longitudinal permanent ground deformation. *In Pipelines 2001: Advances in Pipelines Engineering and Construction*, 1-11.
- Nourzadeh, D.D., Mortazavi, P., Ghalandarzadeh, A., Takada, S., & Ahmadi, M. (2019). Performance assessment of the Greater Tehran Area buried gas distribution pipeline network under liquefaction. *Soil Dynamics and Earthquake Engineering, 124*, 16-34.
- O'Rourke, T.D., & Lane, P.A. (1989). *Liquefaction Hazards and Their Effects on Buried Pipelines*.
- Otsubo, M., Towhata, I., Hayashida, T., Shimura, M., Uchimura, T., Liu, B., ... & Rattetz, H. (2016). Shaking table tests on mitigation of liquefaction vulnerability for existing embedded lifelines. *Soils*

and Foundations, 56(3), 348-364.

Papadimitriou, A.G., Bouckovalas, G.D., Nyman, D. J., & Valsamis, A.I. (2019). Analysis of buried steel pipelines at watercourse crossings under liquefaction-induced lateral spreading. *Soil Dynamics and Earthquake Engineering*, 126, 105772.

Qiao, L., Yuan, C., Miyajima, M., & Zhai, E. (2008). Shake-table testing and FLAC modeling of liquefaction-induced slope failure and damage to buried pipelines. *In Geotechnical Earthquake Engineering and Soil Dynamics, IV*, 1-10.

Sun, H., Miyajima, M., & Qiao, L. (2009). *Buried Pipeline Damage Caused by Soil Liquefaction under the Slope*, 40, 59-64.